

Quantum versus semiclassical description of self-trapping: Anharmonic effects

S. Raghavan*

International Centre for Theoretical Physics, 34100 Trieste, Italy

A. R. Bishop

Los Alamos National Laboratory, Los Alamos, New Mexico 87545

V. M. Kenkre

Center for Advanced Studies and Department of Physics & Astronomy, University of New Mexico, Albuquerque, New Mexico 87131

(Received 22 September 1998)

Self-trapping has been traditionally studied on the assumption that quasiparticles interact with harmonic phonons and that this interaction is linear in the displacement of the phonon. To complement recent semiclassical studies of anharmonicity and nonlinearity in this context, we present below a fully quantum-mechanical analysis of a two-site system, where the oscillator is described by a tunably anharmonic potential, with a square well with infinite walls and the harmonic potential as its extreme limits, and wherein the interaction is nonlinear in the oscillator displacement. We find that even highly anharmonic polarons behave similar to their harmonic counterparts in that self-trapping is preserved for long times in the limit of strong coupling, and that the polaronic tunneling time scale depends exponentially on the polaron binding energy. Further, in agreement, with earlier results related to harmonic polarons, the semiclassical approximation agrees with the full quantum result in the massive oscillator limit of small oscillator frequency and strong quasiparticle-oscillator coupling. [S0163-1829(99)02815-5]

I. INTRODUCTION

Recent work by Grigolini and co-workers,¹ and by Salkola and the present authors,^{2,3} have uncovered subtle features associated with selftrapping of quasiparticles in interaction with vibrations. The vibrations considered in all those analyses have been harmonic. The question of how polaron dynamics and self-trapping are affected by anharmonicities in the vibrations was raised by Kenkre⁴ several years ago at the level of the discrete nonlinear Schrödinger equation (DNLSE) and analyzed in the context of rotational polarons,^{4,5} exponential saturation,^{6,7} and general considerations.⁷ Since the validity of the DNLSE has been called into question by recent considerations,¹⁻³ it is important to examine the issue of what polarons, or selftrapping, owe to harmonic features from a starting point, which is fully quantum. The present paper is devoted to such an examination for a two-site system.

We will focus here on confined systems rather than on periodic systems such as those that may lead to rotational polarons.^{4,7} In a certain sense, the most anharmonic potential conceivable is that which corresponds to a box with infinitely high walls as it corresponds to a harmonic piece with vanishing frequency throughout the interior of the box but one with infinite frequency at the wall. We choose the symmetric Pöschl-Teller potential given by

$$V_{PT}(x) = U_0 \tan^2(ax), \quad (1)$$

because it allows continuous transition between the harmonic oscillator and the box limits and because it can be treated analytically with ease. In Eq. (1) U_0, a are constants defining, respectively, the strength and confining region of the potential. The potential becomes infinitely steep at $x = \pm \pi/2a$. By rewriting the strength of the potential U_0 as

$\lambda(\lambda - 1)\hbar^2 a^2/2m$, where m is the mass of the particle, we introduce the parameter λ , which describes the departure of the potential between the box and harmonic oscillator limits. In the limit $\lambda \rightarrow 1$, the Pöschl-Teller potential becomes the infinite square well of width π/a . In the opposite limit $\lambda \rightarrow \infty$, $a \rightarrow 0$, λa^2 remaining constant (and finite), one recovers the harmonic oscillator potential. The eigenenergies of the Pöschl-Teller potential (1) are given by⁸

$$E_n = \frac{\hbar^2 a^2}{2m} (n^2 + 2n\lambda + \lambda), \quad n = 0, 1, 2, \dots \quad (2)$$

and the corresponding eigenfunctions are

$$\phi_n(x) \equiv \langle x | \phi_n \rangle = N_n \cos^{1/2} ax P_{n+\lambda-1/2}^{1/2-\lambda}(\sin ax), \quad (3)$$

where $P_a^\beta(t)$ are the associated Legendre functions, with $N_n = [a(n+\lambda)\Gamma(n+2\lambda)/\Gamma(n+1)]^{1/2}$.

II. ANHARMONIC POLARON-STATIONARY ASPECTS

Consider a two-site system consisting of a quasiparticle, like an electron or an exciton, whose intersite hopping is described by a matrix element of strength V . The quasiparticle also strongly interacts with a vibrational mode between the two sites. This vibrational mode is described by the Pöschl-Teller potential (1). In the harmonic case the usual interaction is linear in the vibrational amplitude and consequently connects nearest-neighbor eigenstates of the oscillator. These two features are distinct from each other. In developing a scheme for analyzing effects of a generalization to anharmonic situations, we must maintain either one or the other of the two features. We have studied both cases. Here, we present results of maintaining the second feature, viz., an

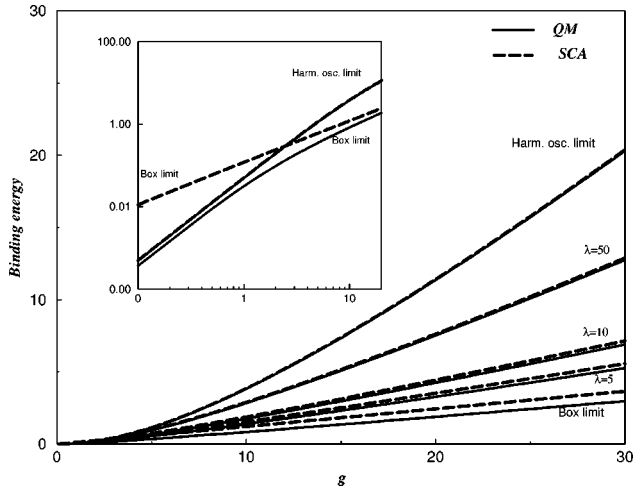


FIG. 1. Polaron binding energy as a function of the quasiparticle-oscillator coupling constant g . The inset shows the same quantities on a logarithmic scale. The solid line indicates the quantum-mechanical result whereas the dashed line indicates the result of the semiclassical approximation (SCA).

interaction that joins nearest-neighbor energy eigenstates. As Nieto and Simmons⁸ and Crawford and Vrcsay⁹ have pointed out in a different context, a sinusoidal interaction possesses this feature for the Pöschl-Teller potential, and also reduces to the linear form in the harmonic limit. We thus take the full Hamiltonian of our system to be

$$H = \frac{\omega_0}{2(\lambda + 1/2)} [\hat{\pi}_z^2 + \lambda(\lambda - 1)\tan^2 \hat{z}] + \omega_0 g \sqrt{\lambda + \frac{1}{2}} \hat{p} \times \sin \hat{z} + V \hat{r}, \quad (4)$$

where

$$\omega_0 = \frac{a^2}{m} \left(\lambda + \frac{1}{2}\right) \quad (5)$$

is the difference between the energies of the first excited state and the ground state of the Pöschl-Teller potential, z is the dimensionless oscillator coordinate ax , and g is the quasiparticle-oscillator coupling constant. Here and henceforth, we put $\hbar=1$ for simplicity.

The operators \hat{p}, \hat{r} are the operators describing the quasiparticle, with $\hat{p} = c_1^\dagger c_1 - c_2^\dagger c_2$, $\hat{r} = (c_1^\dagger c_2 + c_2^\dagger c_1)$, where the c 's are quasiparticle creation and destruction operators. The factorization or the semiclassical approximation (SCA) consists of assuming, equivalently, that the oscillator operators behave classically or that products of quasiparticle-oscillator operators can be factorized.

We compare the SCA with the fully quantum-mechanical results first by computing the polaron binding energies. This is done easily in the strong-coupling limit by freezing the quasiparticle hopping dynamics. We note first that, in the harmonic oscillator limit, the polaron binding energy is proportional to g^2 whereas, in the opposite limit of the infinite square well, the width of the well remains finite and the interaction produces a lowering of energy that is proportional to g . This cross-over behavior becomes evident from the full quantum-mechanical calculations as shown in Fig. 1. Plotted

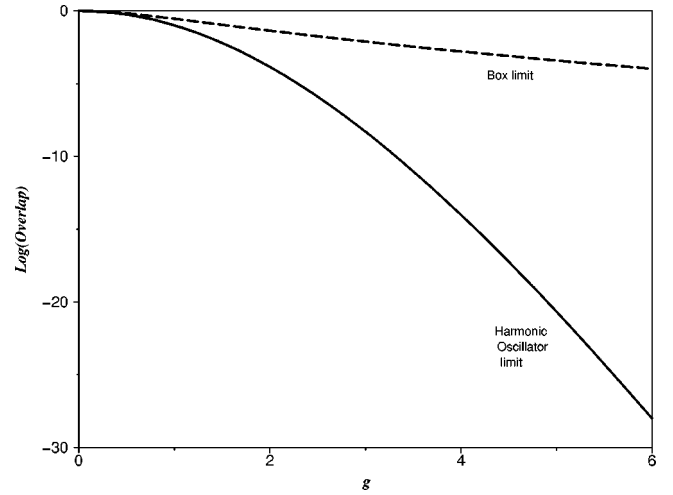


FIG. 2. The overlap of the adiabatically displaced ground-state wave functions plotted logarithmically as a function of g for box limit, $\lambda=1$ (dashed line) and harmonic oscillator limit, $\lambda \rightarrow \infty$ (solid line).

in the main figure is the binding energy (in arbitrary units) as a function of g . In the inset, the same quantities are plotted on a logarithmic scale. The bold lines indicate the fully quantum-mechanical calculation and the dashed lines indicate the results of the SCA. In all the cases, the oscillator frequency ω_0 has been kept fixed, and λ varied allowing the oscillator to pass smoothly from the box ($\lambda=1$) limit to the harmonic ($\lambda \rightarrow \infty$) limit. Two key results are evident in Fig. 1. First, the SCA results agree with the exact ones only in the harmonic oscillator limit; in the square-well limit, the departure becomes quite drastic. Second (see inset), when the system is in the box-limit ($\lambda=1$), the fully quantum system behaves harmonically for small g but exhibits a crossover for larger values of g showing the true box-limit slope of unity.

We also calculate the overlap between the adiabatically displaced ground-state wave functions. This overlap, basically the Huang-Rhys factor, governs the polaronic tunneling rate in the strong-coupling limit. One knows, for instance, that in the harmonic oscillator limit, the tunneling rate is proportional to e^{-g^2} . In Fig. 2, we plot the overlap factor (logarithmically) as a function of g for the box limit, i.e., $\lambda=1$ (dashed line), and for the harmonic oscillator limit, i.e., $\lambda \rightarrow \infty$ (solid line). The quadratic dependence is clearly seen for the latter. However, for $\lambda=1$, the rise is sublinear, showing that the dependence of the overlap factor on g is much weaker.

III. HEISENBERG EQUATIONS

We discuss in this section the temporal evolution of the system, and show how the SCA differs from the fully quantum-mechanical treatment. The equations of motion corresponding to the Hamiltonian (4) can be written as

$$\dot{\hat{p}} = 2V\hat{q}, \quad (6a)$$

$$\dot{\hat{q}} = -2V\hat{p} + 2\omega_0 g(\lambda + 1/2)^{1/2} \hat{r} \sin \hat{z}, \quad (6b)$$

$$\dot{\hat{r}} = -2\omega_0 g(\lambda + 1/2)^{1/2} \hat{q} \sin \hat{z}, \quad (6c)$$

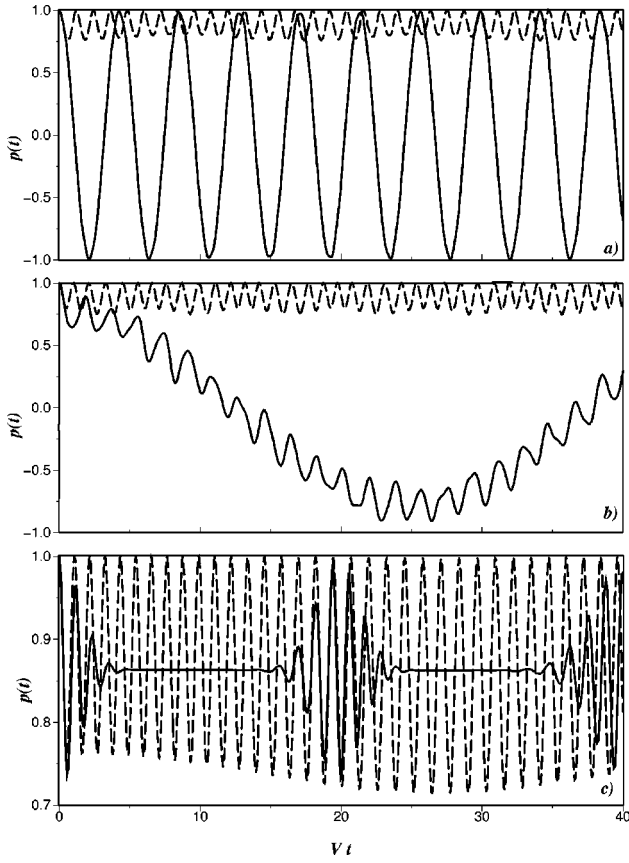


FIG. 3. The evolution of the quasiparticle probability difference $p(t)$ as a function of dimensionless time Vt . In all the figures, the polaron binding energy has been kept fixed at 1.5 V and $\lambda \rightarrow \infty$. The solid line denotes the fully quantum-mechanical result and the dashed line denotes the result of the SCA. In (a) $\omega_0 = 10V$, (b) $\omega_0 = V$, (c) $\omega_0 = 0.1V$.

$$\dot{\hat{z}} = \frac{\omega_0}{(\lambda + 1/2)} \hat{\pi}_z, \quad (6d)$$

$$\dot{\hat{\pi}}_z = -\omega_0 \left[\frac{\lambda(\lambda - 1)}{(\lambda + 1/2)} \tan \hat{z} \sec^2 \hat{z} + g(\lambda + 1/2)^{1/2} \hat{p} \cos \hat{z} \right], \quad (6e)$$

where $\hat{q} = i(c_1^\dagger c_2 - c_2^\dagger c_1)$ and the quasiparticle operators $\hat{p}, \hat{q}, \hat{r}$ cyclically satisfy the commutation relations, $[\hat{p}, \hat{q}] = 2i\hat{r}$, and $[\hat{z}, \hat{\pi}_z] = i$. As stated earlier, the SCA consists in assuming the oscillator operators $\hat{z}, \hat{\pi}_z$ to be c numbers. In the temporal analysis, we compare the results of such an approximation with those given by the full quantum evolution described by Eq. (6). We plot in Figs. 3–5, the evolution of the population difference of the quasiparticle between the two sites $p(t)$ as a function of dimensionless time Vt . In all our calculations, the initial condition used for the quantum system is the ground state of the quasiparticle-oscillator system projected onto the one-site localized part of the Hilbert space, such that $\langle \hat{p} \rangle(0) = 1$. The initial condition used for the SCA calculation is $p(0) = 1$, $\dot{z}(0) = \dot{\pi}_z(0) = 0$. In all the plots, the solid line indicates the full quantum evolution and the dashed line indicates the evolution due to the SCA. The polaron binding energy has been kept constant to facilitate comparison. This value (which we take to be 1.5 V) equals

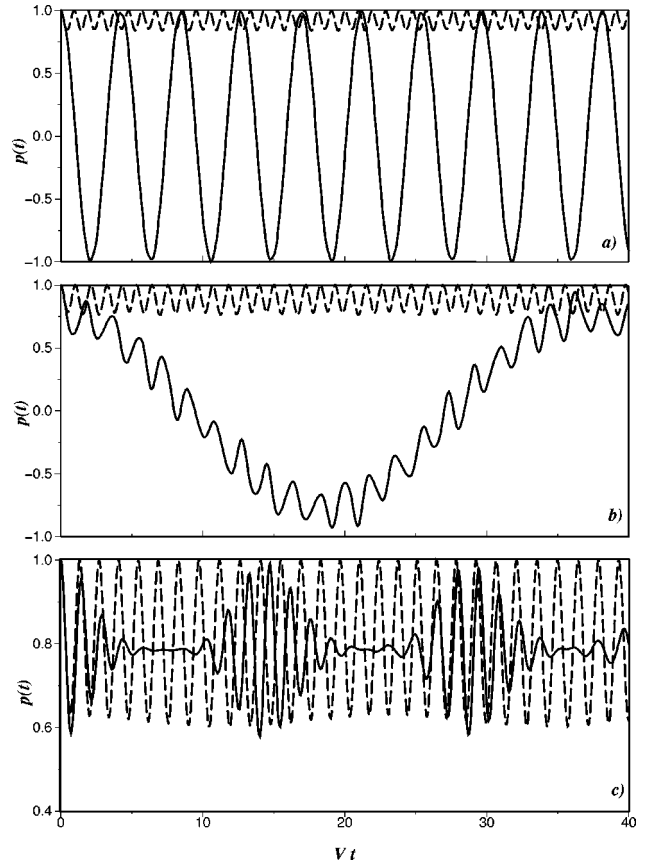


FIG. 4. Same as Fig. 3, with $\lambda = 10$.

$g^2 \omega_0 / 2$ in the harmonic oscillator limit. In Fig. 3, $\lambda = 200$, the oscillator potential is essentially that of the harmonic oscillator potential. The oscillator energy ω_0 takes on the values 10V, V, and 0.1V in (a), (b), and (c), respectively. As discussed elsewhere,² whereas the SCA shows self-trapping for all the values of the oscillator frequency, the full quantum evolution differs substantially, except in the limit of low-oscillator energy $\omega_0 = 0.1V$. In this limit, for short times, the full quantum evolution and SCA agree in that both show self-trapping, with nearly the same average value of self-trapping and oscillation frequency. However, the quantum evolution shows a considerably richer structure involving collapses and revivals. At much longer times, the dressed quasiparticle tunnels from one site to the other. This is evident in Fig. 3(b). When $\lambda = 10$, (Fig. 4), the potential is more ‘‘square-well’’-like and some departures, especially in the small oscillator frequency regime [Fig. 4(b)] are visible. For instance, the ‘‘silent runs’’ separating the collapse and revival sequence, are less quiescent, and the agreement between the SCA and the full quantum evolution is slightly worse. In Fig. 5, we take $\lambda = 1$, wherein the potential is essentially the infinite square well. Whereas the agreement between the SCA and the full quantum evolution is best when the oscillator energy is least, $\omega_0 = 0.1V$, [Fig. 5(c)], the agreement is far worse than for the harmonic potential [Fig. 5(c)]. Further, the ‘‘silent runs’’ are barely noticeable, with the collapses and revivals intruding into each other.

A key time scale in the temporal evolution is the one associated with the polaronic tunneling between the two sites. Since this time scale is intimately connected with the

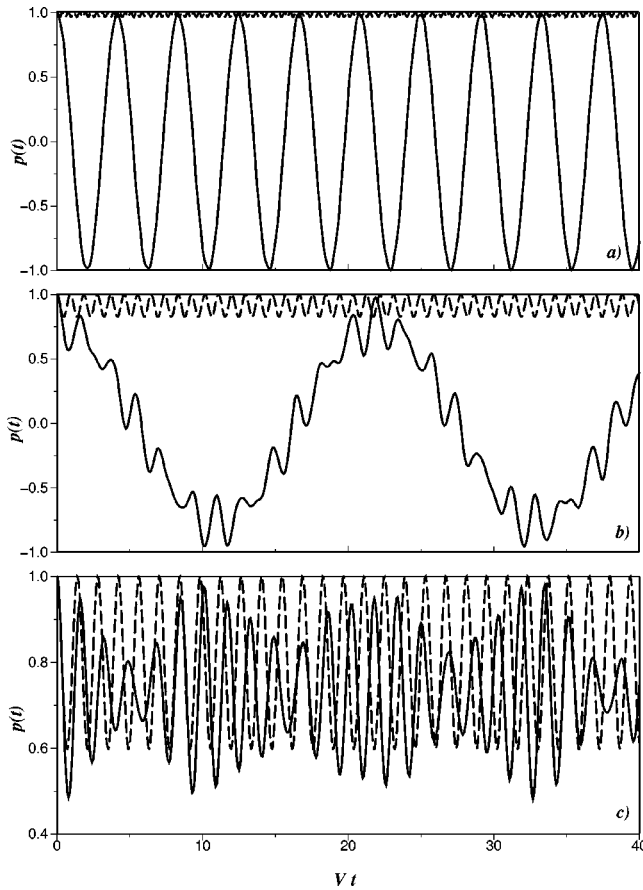


FIG. 5. Same as Fig. 3, with $\lambda=1$.

polaron binding energy, we plot in Fig. 6, the logarithm of the tunneling time as a function of the binding energy. The solid line denotes the harmonic oscillator limit $\lambda \rightarrow \infty$ whereas the dashed line denotes the infinite square-well limit, $\lambda=1$. Note that for small values of the binding energy, the timescales for both cases is only weakly dependent on the energy. However, for larger coupling (binding energy), both show a clear linear dependence (albeit with different slope). This clearly indicates that even for the boxlike potential, the polaronic tunneling time scale is exponentially dependent on the binding energy. While well known for harmonic polarons, this exponential dependence constitutes an important new result for anharmonic polarons emerging from the present analysis.

*Present address: Rochester Theory Center for Optical Science and Engineering, Department of Physics & Astronomy, University of Rochester, Rochester, NY 14627.

¹P. Grigolini, *Int. J. Mod. Phys. B* **6**, 171 (1992); L. Bonci, P. Grigolini, and R. Roncaglia, *Phys. Rev. A* **47**, 3538 (1993); L. Bonci, R. Roncaglia, B.J. West, and P. Grigolini, *ibid.* **45**, 8490 (1992); D. Vitali and P. Grigolini, *ibid.* **42**, 7091 (1990); D. Vitali, P. Allegrini, and P. Grigolini, *Chem. Phys.* **180**, 297 (1994).

²M.I. Salkola, A.R. Bishop, V.M. Kenkre, and S. Raghavan, *Phys. Rev. B* **52**, R3824 (1995).

³V.M. Kenkre, S. Raghavan, A.R. Bishop, and M.I. Salkola, *Phys. Rev. B* **53**, 5407 (1996); S. Raghavan, V.M. Kenkre, A.R. Bishop, and M.I. Salkola, *ibid.* **53**, 8457 (1996).

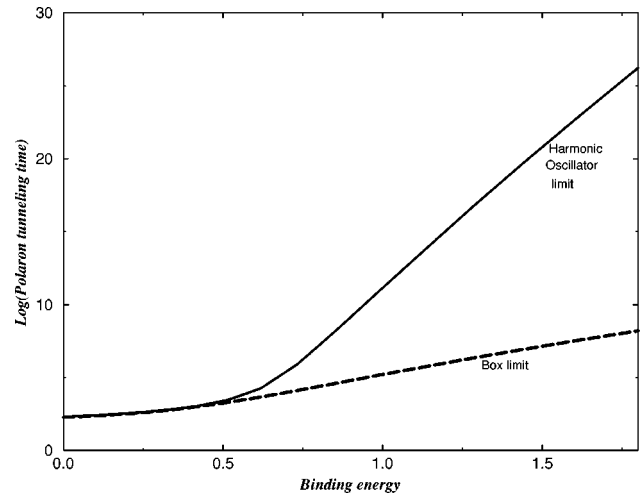


FIG. 6. The polaron tunneling time scale plotted logarithmically as a function of the polaron binding energy, both computed without making the SCA. The solid line indicates $\lambda \rightarrow \infty$ (harmonic oscillator limit) and the dashed line indicates $\lambda=1$ (box limit).

IV. SUMMARY

By analyzing the dynamics and energetics of a quasiparticle interacting with a tunably anharmonic oscillator, specifically described by a Pöschl-Teller potential, we find that, in the limit of strong coupling between the quasiparticle and the oscillator, self-trapping is robust and persists for strong anharmonicities, with the polaron tunneling time scale being exponentially dependent on the polaron binding energy, a feature that has been earlier known to be true for harmonic polarons. We further find that the full quantum result agrees with the predictions of the semiclassical approximation only in this strong coupling, low-frequency regime, in agreement with earlier findings for harmonic polarons.

ACKNOWLEDGMENTS

One of us (V.M.K.) acknowledges the financial support of the National Science Foundation under Grant No. DMR-9614848, and of the Los Alamos National Laboratory under Grant No. 0409J0004-3P.

⁴V.M. Kenkre, in *Singular Behavior and Nonlinear Dynamics*, edited by S. Pnevmatikos, T. Bountis, and S. Pnevmatikos (World Scientific, Singapore, 1989).

⁵V.M. Kenkre, H.-L. Wu, and I. Howard, *Phys. Rev. B* **51**, 15 841 (1995); H.-L. Wu and V.M. Kenkre, *Phys. Lett. A* **199**, 61 (1995).

⁶V.M. Kenkre, M.F. Jørgensen, and P.L. Christiansen, *Physica D* **90**, 280 (1996).

⁷V.M. Kenkre, *Physica D* **113**, 233 (1998); S. Raghavan, *Phys. Lett. A* **235**, 48 (1997); R. Amritkar and V.M. Kenkre (unpublished).

⁸M.M. Nieto and L.M. Simmons, Jr., *Phys. Rev. D* **20**, 1332 (1979).

⁹M.G.A. Crawford and E.R. Vrscaj, *Phys. Rev. A* **57**, 106 (1998).